Pattern Formation in Homogeneous Polymer Solutions Induced by a Continuous-Wave Visible Laser

R. Sigel,[1]* G. Fytas,[1,2]† N. Vainos,[1]‡ S. Pispas,[3]
N. Hadjichristidis[3]

We report an unexpected nonphotothermal material organization induced by continuous-wave visible laser light at low power levels. This effect is observed along the laser beam propagation direction in fully transparent entangled solutions of common homopolymers featuring sufficiently high molecular mass and optical anisotropy along the chain backbone. The resulting formation of long-lived stringlike or dotlike patterns on the micrometer scale, probed by dark-field coherent imaging, depends on the molecular mass, architecture, solvent nature, and polymer concentration. Electrostrictive and alignment forces as well as chain cooperativity are responsible for the osmotic compression of the polymer solute. Subsequent waveguiding effects induce autoamplification and "pattern writing" upon prolonged illumination. This wave-medium coupling could potentially lead to photorefractive, microoptics, and nanotechnology applications.

The interactions of light with matter have extreme scientific and technological importance. Tightly focused laser beams are able to trap dielectric particles and immobilize against Brownian motion, gravity, and convection and have opened the route to molecular object manipulation (*1–6*). For slightly focused, low-intensity laser light, propagating in a transparent medium, the phenomenon of scattering can be observed, which reflects the materials structure and dynamics; nonlinear optical effects can be observed at high illumination intensities.

At concentrations c higher than the overlap concentration c^*, polymer coils are in the semidilute regime and exhibit substantial interpenetration of the individual polymer chains. Because of weak concentration fluctuations, these solutions (*7*) scatter weakly visible laser light. In the experimental configuration of Fig. 1, this situation is visualized by observing a fully transmitted coherent beam (**1**) on the screen and a smooth beam trace (due to scattered light) viewed by the charge-coupled device (CCD) camera perpendicular to the beam axis. This is the case when using, for example, a semidilute solution of polystyrene (PS) $[\text{-CH}_2\text{-CH (C}_6\text{H}_5\text{)-}]_N$ ($N = 9600$) in toluene at a concentration of $c = 0.04$ g/ml.

In contrast, a semidilute solution of a poly(isoprene-1,4) (PI) $[\text{-H}_2\text{C-C (CH}_3\text{)=CH-CH}_2\text{-}]_N$ ($N = 17{,}060$) in *n*-hexane demonstrates dramatically different behavior. For $c = 0.023$ g/ml and with the use of a red krypton-ion laser beam (wavelength $\lambda = 647$ nm) at power $P_0 = 100$ mW, effects such as those depicted in Fig. 2, A to D, are observed. The initially well-defined Gaussian profile of the transmitted beam (Fig. 2A) projected on the screen widens up to a richly structured pattern (Fig. 2B), which fluctuates over several minutes and stabilizes thereafter while under laser illumination. Simultaneously, the initially smooth trace of the scattered light (Fig. 2C) becomes brighter and exhibits a transient flashing behavior (Fig. 2D). By blocking the laser beam (**1**) and using the attenuated illumination beam (**2**), dark-field coherent imaging of the solution clearly reveals a stable "written" pattern in the solution along the propagation direction of the laser beam. Both stringlike and dotlike structures (Fig. 2, E and F) were formed using polymer solutions of different characteristics as described below. Changes in the spot of the transmitted beam appear on the screen much earlier than the definite formation of written structures. The incubation time (5 to 400 s) for the onset of the transmitted beam widening was found to vary linearly with $1/P_0$ in the range from 2 to 150 mW. This observation indicates a linear optical exposure dependence. The described pattern formation is absent when lens L_1 (Fig. 1) is removed; that is, for an unfocused incident laser beam.

To study this unexpected effect, we first examined its appearance in relation to the refractive index difference between polymeric solute (n_p) and solvent (n_s). Comparing solutions of PI ($n_p = 1.51$) in different solvents [*n*-hexane ($n_s = 1.37$), cyclohexane ($n_s = 1.43$), toluene ($n_s = 1.49$), and bromoform ($n_s = 1.60$)] at the same volume concentration of PI, the effect strengthens with increasing $n_p - n_s$ and is absent for $n_p - n_s < 0$ (such as in bromoform).

This distinct wave-medium coupling in semidilute solutions of PI may relate to the substantial contribution of the double bond to the polarizability anisotropy along the chain backbone (*8*). Such a proposition appears to be supported by the similar behavior observed in semidilute solutions of 1,4-polybutadiene (1,4-PB) $(\text{-CH}_2\text{-HC=CH-CH}_2\text{-})_N$ ($N = 18{,}520$; $n = 1.51$) in *n*-hexane for $c > 0.016$ g/ml. Consequently, the normal neutral behavior of PS would imply that the polarizability anisotropy in the main chain (backbone) is a necessary condition. To check this conjecture, we compared the behavior of 1,4-PB ($N = 3060$) and 1,2 PB $[\text{-CH}_2\text{-CH(CH=CH}_2\text{)-}]_N$ ($N = 3780$) with the double bond on the chain backbone and the side group, respectively. Although a clear stringlike pattern is written in 1,4-PB, the effect is absent in 1,2-PB, even at the highest examined concentration ($c = 0.15$ g/ml).

Figure 3 shows the minimum critical concentration c_c above which the profile of the transmitted laser beam definitely changes

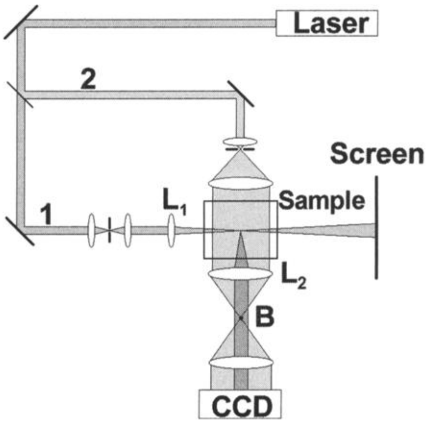

Fig. 1. Schematic drawing of the experimental setup. The main beam (**1**) of a red continuous-wave krypton-ion laser ($\lambda = 647$ nm) is spatially filtered and focused by lens L_1 (f = 100 mm) into the rectangular optical cell (1 cm × 1 cm) containing the polymer solution. Modifications of the profile of the transmitted laser beam are directly observed on the screen. The laser beam trace in the solution is magnified by a microscope optical arrangement and recorded by a CCD camera. A low-power (~5% of the total available power) split or separately produced beam (**2**) is used to illuminate the sample in a dark-field coherent imaging arrangement, using a high-pass filtering stop (B) at the focal plane of the objective lens L_2.

---

[1] FO.R.T.H.-Institute of Electronic Structure and Laser, Post Office Box 1527, 71110 Heraklion, Crete, Greece. [2] Max Planck Institute for Polymer Research, Post Office Box 3148, 55021 Mainz, Germany. [3] Department of Chemistry, University of Athens, 15701 Athens, Greece.

*Present address: Max Planck Institute of Colloids and Interfaces, Am Muehlenberg 1, 14476 Golm, Germany.

†To whom correspondence should be addressed. E-mail: fytas@iesl.forth.gr

‡Present address: National Hellenic Research Foundation–Theoretical and Physical Chemistry Institute, 48 Vas. Constantinou Avenue, 11635 Athens, Greece.

into a complex pattern on the screen (Fig. 2) as a function of N. The value of this cutoff concentration appears to be insensitive to laser power and displays the scaling $N^{-0.8\pm0.1}$ validated for both PI and PB in *n*-hexane. This relationship resembles that of the overlap concentration c^*(*7*), and the absolute value is on the order of the entanglement concentration (~10 c^*). Rheological measurements on these solutions revealed a rubberlike plateau in the dynamic shear modulus characteristic of a temporary entangled polymer network. Short chains dilute an entangled network, and consequently a symmetric (50:50) mixture of short ($N = 1910$) and long ($N = 17{,}060$) PI chains (PI mixture in Fig. 3) exhibits a higher c_c value as compared to the c_c value expected for PI chains with the average N (~9500). It is not, therefore, the total polymer concentration but rather the chain connectivity that determines the critical value c_c. This notion is further corroborated by the behavior of the multiarm star PB, which has a lower overlap concentration c^* than does the corresponding linear PB. Based on the scaling of Fig. 3, no effect would be expected below a certain threshold N_c (~150), nearly equal to the chain length above which bulk PI becomes entangled. This prediction has been experimentally verified for a PI ($N = 70$)/*n*-hexane solution at concentrations up to the bulk state.

Written patterns such as those depicted in Fig. 2, E and F, are polymer-rich stable regions. Their optical detection is based on the existence of an optical dielectric contrast ($n_p - n_s > 0$); at c_c no written pattern was detected and higher concentrations were needed. The evolution of the laser beam trace in the solution (Fig. 2, C and D) and the dynamic pattern formation indicate that the laser-induced enhancement of the polymer concentration exerts optical focusing and waveguiding actions on the laser beam itself, thereby yielding autoamplification of the observed phenomena. In fact, the burstlike appearance of Fig. 2D hints at leaky waveguiding modes due to inhomogeneous field confinement.

The observed refractive index variation is clearly unrelated to well-known dynamic nonlinear optical (Kerr) and thermal blooming effects, but it is definitely based on mass transfer and reversible (stable) pattern formation (*9*). On the other hand, laser-generated temperature gradients may cause concentration variations due to the photothermal mechanism (*10–12*). In this case, the flow direction of the solute depends on the sign of the thermodiffusion coefficient. In the present systems, however, there is no measurable absorption, and thus the photothermal effects should be inactive. In addition, the positive thermodiffusion coefficient of the present PI solutions (*13*) would result in the motion of the polymer solute toward the cold region; that is, outside the laser beam interaction volume, in contrast to the present observations.

Electric field (E) gradients of a focused laser light are also known to exert radiation forces (*1*, *2*) that can immobilize particles against Brownian motion if $n_p - n_s > 0$. Such radiation forces can, for example, draw microspheres into regions of high intensity and produce artificial Kerr media, which enable self-focusing of the laser beam (*14*, *15*). For efficient trapping, the potential of the gradient force $U = n_p \alpha E^2/2$ must exceed the thermal energy kT. Using a typical value for the polarizability α (~10×10^{-24} cm^3) per monomer unit and $E^2 \sim (8\pi/c)P_0/\sigma$ (where c is the speed of light and $\sigma \sim 10^{-5}$ cm^2 is the cross-sectional area of the focused laser beam), the trapping potential U is found to be eight to nine orders of magnitude less than kT. This rough estimate rationalizes the nontrapping behavior of all polymers used so far. In the present case of the polyolefins (PI and PB), however, in which the new effect is observed, the above estimate shows that independent and single optically anisotropic double bonds also cannot provide sufficient force for trapping (*16*). Therefore, beyond the classical interpretation of radiation pressure, cooperativity must be an essential feature of the present wave-medium interactions in the notion of chain topological constraints. The involvement of the macromolecular chains in the entangled network is confirmed by the effects observed in the mixture of short and long PI chains and the comparison between linear and multiarm star PB (Fig. 3).

The rate of material condensation in the laser field speeds up with polymer concentration, and the associated incubation time decreases approximately as c^{-1}. Because of the

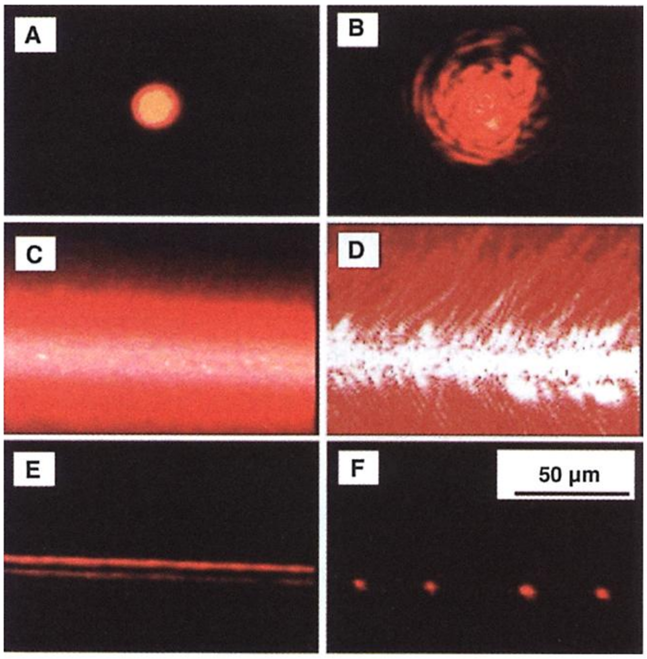

Fig. 2. Images of the laser beam observed on the screen (**A** and **B**) and the laser beam trace in the solution observed perpendicularly (**C** and **D**). Written refractive index patterns (**E** and **F**) were observed by dark-field coherent imaging (with the transmitted laser beam blocked). [(A) and (C)] and [(B) and (D)] refer to early and late instants of laser medium interaction, respectively. (C) to (F) are recorded for semidilute solutions of PI (N = 17060) in n-hexane (c = 0.03 g/ml) and toluene (c = 0.034 g/ml), respectively. The apparent tubelike pattern of (E) arises from a single dense string because of a refractive index gradient on both sides. The scale bar in (F) refers to (C) to (F) and highlights the shorter dimensions of the actual written pattern [(E) and (F)] as compared to the beam waist in the medium (C).

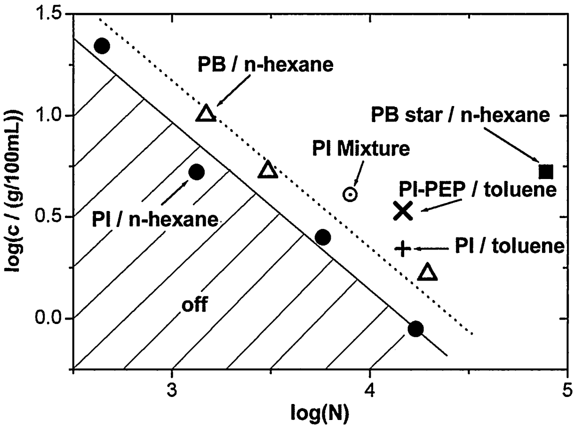

Fig. 3. Critical minimum concentration c_c (in grams per 100 ml) versus the number of monomer units N necessary to observe changes in the transmitted beam (Fig. 2, A and B) through the indicated semidilute polymer solutions. The solid line represents a linear fit of the PI/n-hexane system. "PI mixture" stands for a symmetric mixture of a low (N = 1910) and high (N = 17,060) molar mass PI in n-hexane, and its c_c value falls well above the solid line because of the reduced number of entanglements. The dotted line indicates a linear fit of the PB/n-hexane system.

enhanced osmotic pressure, concentration changes occur rapidly via cooperative diffusion; with a cooperative diffusion coefficient $D_c \sim 10^{-6}$ cm^2/s (*7*), the solvent can be expelled from the focal spot ($L \simeq 10$ μm) in less than 1 s. Once the patterns are formed, they fade out extremely slowly with a time constant τ on the order of days. The lifetime is estimated as $\tau \simeq L^2/D$ with a diffusion coefficient $D = kT/(6\pi\eta R)$ (η is the solution viscosity and R the lateral size of the optical pattern).

The writing process leading to the spatial pattern formation is the result of the prolonged interaction of the incident laser beam with local regions of higher polymer concentration and hence higher refractive index. The speckle-like picture of the transmitted beam (Fig. 2B) is owing to the propagation effects through a cylindrical waveguiding structure exhibiting spatial refractive index inhomogeneities. Investigations using polarized light (both linear and circular) revealed no variation in the formation of the optical structures of Fig. 2, E and F. Furthermore, the use of crossed polarizers in the imaging optics (branch **2** in Fig. 1) revealed no measurable birefringence, thus suggesting a negligible chain alignment along the laser beam propagation axis. This effect bears no analogy to the extensional and aligning effect of elongational flow fields (*17*). The polymer chains are probably oriented radially toward the strings, and the presence of an entangled network might further enhance this orientation because of local mechanical stress.

The wave-medium coupling in the polyolefins is also influenced by the macromolecular architecture. A linear PB ($N = 3060$) and a multiarm star (*18*) PB 6480 ($N = 77{,}780$) were selected because they have the same monomer structure but a vastly different total number of monomers. Nevertheless, both samples in *n*-hexane exhibit similar $c_c \simeq 0.06$ g/ml (Fig. 3). At $c \simeq 0.11$ g/ml, the dotted structure for the multiarm star PB 6480 is much weaker than the one observed in the linear PB solution; whereas at higher concentrations, stringlike structures are observed for both. These structures are visualized in Fig. 4 along with the pronounced stringlike pattern in PB ($N = 18{,}150$) at 0.04 g/ml. The radiation force exerted on these chemically similar systems is obviously different, and the star topology apparently affects the c_c-N plot of Fig. 3. However, the PB star conforms to the c_c-N scaling of the linear PB when its lower overlap concentration c^* (*18*) is taken into account; as, for example, in a c_c/c^*-N plot. The location in the c_c-N plot also depends on the concentration of the -C=C- bonds in the chain. Partial (~55%) hydrogenation of PI to a block poly(isoprene-*r*-ethyl propylene) (PEP) increases c_c relative to the parent PI (Fig. 3). Although a dotlike pattern is written in PI/toluene at 0.036 g/ml, no structure is formed in the PEP/toluene solution.

To determine whether chemical modification was an issue, a PI/*n*-hexane solution (0.1 g/ml) in a small volume (~50 μL) was illuminated by a $\lambda = 647$ nm laser beam at a power level of $P_0 = 200$ mW for several hours, thus inducing extensive pattern formation. No detectable change in the narrow molecular weight distribution of PI was observed independent of the amount of the added antioxidant (radical trap) used. ^{1}H– and ^{13}C–nuclear magnetic resonance analysis also excluded cis-trans (*19*) chain isomerization. Furthermore, the effect induced by shorter wavelength light ($\lambda = 532$ nm) was unexpectedly (for classical trapping) found to be weaker (*20*). Bearing in mind the large absorption of the used polymers in the ultraviolet spectral range, this finding along with the linear dependence of the incubation time on $1/P_0$ excludes multiphoton absorption effects.

Long-lived reversible reorganization of entangled polyolefins in organic solvents is induced near the focus of a continuous-wave visible laser beam at low power levels. This optical effect lacks at present a fully satisfactory explanation in the frame of classical electrostriction and aligment. The role of other parameters such as temperature, laser wavelength, and polymer architecture needs to be examined. The richness of polymer chemistry, however, in conjunction with the fundamental phenomena of soft matter manipulation and the potential applicability in optical and nanotechnology systems, offer several perspectives.

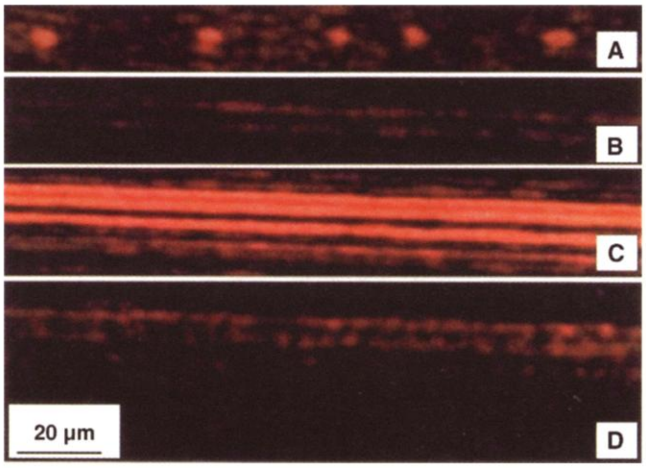

Fig. 4. Dark-field images of the spatial concentration patterns written for 5 min by a slightly focused continuous-wave laser ($\lambda = 647$ nm) in PB in *n*-hexane solutions. Short linear PB ($N = 3060$) at 0.08 g/ml is shown in (**A**) and at 0.11 g/ml in (**B**). Longer linear PB (N = 18,520) is shown at 0.04 g/ml in (**C**). Multiarm star PB6480 ($N = 77{,}780$ with 59 arms) is shown at 0.12 g/ml in (**D**).

References and Notes

1. A. Ashkin, J. M. Dziedzic, T. Yamane, *Nature* **330**, 769 (1987).
2. S. Chu, *Science* **253**, 861 (1991).
3. A. Ashkin, *Proc. Natl. Acad. Sci. U.S.A.* **94**, 4853 (1997).
4. D. Chiu, R. N. Zare, *J. Am. Chem. Soc.* **118**, 6512 (1996).
5. K. Hirano *et al.*, *Appl. Phys. Lett.* **80**, 515 (2002).
6. L. I. McCann, M. Dykman, B. Golding, *Nature* **402**, 785 (1999).
7. P. G. de Gennes, *Scaling Concepts in Polymer Physics* (Cornel Univ. Press, Ithaca, NY, 1979).
8. G. Fytas, G. Floudas, N. Hadjichristidis, *Polym. Comm.* **29**, 322 (1988).
9. Third-order optical nonlinearities (susceptibility $\chi^{(3)}$) in isotropic media yield typically nonlinear refractive index coefficients, $n_2 \propto \chi^{(3)}$, on the order of 10^{-10} cm^2/W to 10^{-12} cm^2/W at best (for absorbing media). For the maximum intensity used here ($I_0 \sim 5 \times 10^4$ W/cm^2, for $P_0 = 100$ mW in the sample), the expected contribution $\Delta n = n_2 I_0 \sim 10^{-7}$ to 10^{-8} would be extremely small and cannot be compared with the observed $\Delta n \sim n_p - n_s \sim 10^{-1}$. Furthermore, thermal blooming effects would also require over 100° temperature rise to give some appreciable effects. Neither the magnitude nor the dynamics of the observed effects can be justified in the frame of the above well-known phenomena.
10. J. Hofkens, J. Hotta, K. Sasaki, H. Masuhara, K. Iwai, *Langmuir* **13**, 414 (1997).
11. J. P. Delville, L. Lalaude, S. Buil, A. Ducasse, *Phys. Rev. E* **59**, 5804 (1999).
12. S. Juodkazis *et al.*, *Nature* **408**, 178 (2000).
13. M. Schimpf, S. Giddings, *J. Polym. Sci.* **B27**, 1317 (1989).
14. A. Ashkin, J. M. Dziedzic, P. W. Smith, *Opt. Lett.* **7**, 276 (1982).
15. It is worth underlining the differences between the artificial Kerr medium described above and in related references as (i) the morphology between the "permanently written" patterns of Fig. 2E and the self-focusing beam trajectory of Fig. 2 in (*14*); (ii) the observed values of $\Delta n \sim 10^{-4}$ [yielding $n_2 \sim 10^{-9}$ (cm^2/W)] for the artificial Kerr medium, against the present $\Delta n \sim 10^{-1}$; and (iii) the largely differing kinetics of the respective phenomena manifested by the fast decay of the trapped microspheres pattern upon removal of the illumination.
16. The large polarizability anisotropy (Δα) per repeating unit along the chain backbone could lead to matter reorganization due to laser field–induced alignment. The estimated monomer order parameter $S \sim E^2\Delta\alpha/kT \sim O(10^{-9})$ is very low in analogy to the insufficient classical trapping.
17. A. Keller, J. A. Odell, *Colloid Polym. Sci.* **263**, 187 (1985).
18. It consists of 59 arms each with $N_a = 1320$ connecting on the same dendritic core [J. Roovers, *Macromolecules* **27**, 5359 (1994)].
19. K. Ichimura, S.-K. Oh, M. Nakagawa, *Science* **288**, 1624 (2000).
20. Weak absorption at 647 nm and hence thermal lensing at this low power level is very unlikely, in agreement with the observed slow kinetics. This wavelength dependence might relate to the viscoelastic nature of the entangled polymer solutions.
21. We thank P. G. de Gennes, G. Wegner, and B. Chu for helpful comments and discussions and D. Vlassopoulos for the rheological measurements. Partial financial support of the Greek Ministry of Education (grant 1090) is gratefully acknowledged.

15 March 2002; accepted 6 May 2002